Accepted Manuscript

Dispersibility and biotransformation of oils with different properties in seawater

Odd G. Brakstad, Umer Farooq, Deni Ribicic, Roman Netzer

PII: S0045-6535(17)31581-3

DOI: 10.1016/j.chemosphere.2017.10.012

Reference: CHEM 20034

To appear in: *ECSN*

Received Date: 7 July 2017

Revised Date: 11 September 2017

Accepted Date: 2 October 2017

Please cite this article as: Brakstad, O.G., Farooq, U., Ribicic, D., Netzer, R., Dispersibility and biotransformation of oils with different properties in seawater, *Chemosphere* (2017), doi: 10.1016/j.chemosphere.2017.10.012.

Dispersibility and biotransformation of oils with different properties in seawater

Authors: Odd G. Brakstad*[A)], Umer Farooq[A)], Deni Ribicic[B)] and Roman Netzer[A)]

[A)]SINTEF Materials and Chemistry, Environmental Technology, Dept. Applied Environmental Biology and Chemistry, N-7465 Trondheim, Norway

[B)]The Norwegian University of Science and Technology, Dept. Cancer Research and Molecular Medicine, N-7491 Trondheim, Norway

Corresponding author: Odd G. Brakstad; e-mail odd.brakstad@sintef.no; Phone +47 98243447; Fax no. +47 73597043

Key words: Oil; dispersants; dispersibility; biodegradation; seawater;

ABSTRACT

Dispersants are used to remove oils slicks from sea surfaces and to generate small oil-droplet dispersions, which may result in enhanced biodegradation of the oil. In this study, dispersibility and biodegradation of chemically dispersed oils with different physical-chemical properties (paraffinic, naphthenic and asphaltenic) were compared in natural temperate SW at 13°C. All selected oils were chemically dispersible when well-known commercial dispersants were used. However, interfacial tension (IFT) studies of the dispersed oils showed different IFT properties of the oil at 13°C, and also different leaching of the dispersants from oil droplet surfaces. Biodegradation studies of the chemically dispersed oils were performed in a carousel system, with initial median droplet sizes < 30 µm and oil concentrations of 2.5-2.8 mg/L. During biodegradation, oil droplet concentrations were rapidly reduced, in association with the emergence of macroscopic 'flocs'. Biotransformation results showed that half-lives of semivolatile total extractable organic carbon (TEOC), single target 2- to 4-ring PAH, and 22 oil compound groups used as input data in the oil spill contingency model OSCAR, did not differ significantly between the oils ($P>0.05$), while *n*-alkanes half-lives differed significantly ($P<0.05$). Biotransformation was associated with rapid microbial growth in all oil dispersions, in association with *n*-alkane and PAH biotransformation. These results have implications for the predictions of biodegradation of oil slicks treated with dispersants in temperate SW.

1. Introduction

The use of chemical dispersants is an important operational tool for treatment of surface or subsurface oil discharges in the marine environment. Dispersants have been used in several oil spill operations (Prince, 2015). Dispersants were also injected subsurface during the *Deepwater Horizon* (DWH) blowout in 2010, to reduce oil surfacing (Atlas and Hazen, 2011; Kujawinski et al., 2011), and subsequent stranding of the oil.

Chemical dispersants are mixtures of surfactants and solvents, creating more hydrophilic oil surfaces, and generating small oil droplets with low rising velocities in the seawater (SW) column (Lessard and DeMarco, 2000; Prince, 2015). Several laboratory studies under different environmental conditions have shown that the use of chemical dispersants promote oil biodegradation (Brakstad et al., 2014; McFarlin et al., 2014; Prince et al., 2013; Siron et al., 1995; Venosa and Holder, 2007; Zahed et al., 2011). However, other studies have suggested no or uncertain effects of dispersants on oil biodegradation after dispersant treatment (Lindstrom and Braddock, 2002; Macnaughton et al., 2003), or even inhibitory impacts of dispersant components on oil biodegradation rates have been suggested (Kleindienst et al., 2015; Rahsepar et al., 2016). Several biodegradation studies of chemically dispersed oil have been performed with unrealistically high concentrations of oil or dispersant, which may limit biodegradation due to nutrient depletion (Lee et al., 2013), or cause prolonged lag-periods due to toxic effects. It was also observed that low oil concentrations resulted in more efficient biodegradation of chemically dispersed oil than high concentrations (Zahed et al., 2010). The surfactant dioctyl sulfosuccinate (DOSS) of the dispersant Corexit 9500, and the hydrocarbon fraction of the dispersant used during the DWH spill, have also been shown to be biodegradable with enrichment cultures from Gulf of Mexico (GoM) SW at 25°C or 5°C (Bælum et al., 2012; Campo et al., 2013).

It is important that the oil is dispersed to small-oil droplet dispersions for efficient biodegradation. It was recently shown that hydrocarbons in oil dispersions with median droplet diameters of 10-30 µm are rapidly biodegraded in Norwegian or GoM, using a fresh paraffinic oil (Brakstad et al., 2014; Brakstad et al., 2015a; Hu et al., 2017; Wang et al., 2016). However, non-dispersed oil emulsions are poorly biodegradable, with the exceptions of oil compounds dissolving to the SW (Brakstad et al., 2014). Slightly weathered emulsions may be dispersible under breaking wave conditions, but the generated droplets are large (> 100 µm) (Daling et al., 2014). Biodegradation of these large droplets is therefore expected to

be poor or negligible (Brakstad et al., 2014). Dispersant treatment will result in breaking of the emulsions at various degrees, resulting in generations of dispersions (Strøm-Kristiansen et al., 1997), and the conditions for biodegradation will be improved.

The ability of an oil to disperse is important for the ability of the oil to biodegrade. The dispersibility of the oil may depend on its physical-chemical properties at different weather and temperature conditions. For instance wax-rich oils have shown poorer dispersibility properties than paraffinic, naphthenic, and asphaltenic oil in SW, especially in cold SW when or the wax solidifies (Strøm-Kristiansen et al., 1997). Data on the dispersibility of an oil are therefore important both for decision of using dispersants after an oil spill, and as a background for predicting its biodegradability after an oil spill.

Dynamic models are used to predict the fate of the oil after a spill, and for the estimation of the efficiency of oil spill operations. One of these models is the three-dimensional OSCAR model (Reed et al., 1995). In this model, experimental biotransformation rates of oil compound groups have been included as part of the fate predictions (Brakstad and Faksness, 2000; Reed et al., 2001). These compound groups represent a boiling point range of ÷160 to > 500°C, covering more than 80 % of most light oils, according to the true boiling point curve (Pasquini and Bueno, 2007). The biodegradation rates used in the OSCAR model were originally derived from paraffinic oils with similar physical properties, using mechanically prepared dispersions (Brakstad and Faksness, 2000). Biodegradation data are therefore required for chemically dispersed oils with different properties, as part of the fate predictions after dispersant oil spill treatment.

The main objective of this study was to compare the dispersibility and biodegradation of North Sea crude oils with different properties, when treated with common commercial chemical dispersants. The selected oils included both paraffinic, naphthenic and asphaltenic oils, and biodegradation was performed in natural SW at a temperature relevant for North Sea summer conditions (13°C). The results from this project would also address if generic rather than oil-specific biodegradation data were needed for oil spill models like OSCAR, when predicting the fate of an oil spill treated with dispersants at conditions relevant for this study.

2. Materials and Methods

2.1 Crude oils, dispersants and seawater

Norwegian crude oils, representing paraffinic (Statfjord C), naphthenic (Troll C) and asphaltenic (Grane) oils were used in this study (Table S1, Supplementary Information). In addition, an expected asphaltenic oil (Balder) proved to be a blend of asphaltenic (40%) and paraffinic (Ringhorne (60%) oils (Table S1). All oils were heated prior to use (50°C, 1 hour) to melt wax generated during storage. Water-in-oil (w/o) emulsions (50 or 75 % SW) of evaporated (250°C) or photo-oxidized (xenon high pressure lamp, IR and UV filters [sunlight conditions]; 20 h) Stafjord C or Troll C oils were prepared in rotating centrifuge funnels as previously described (Daling et al., 1990). Properties of fresh and evaporated/photo-oxidized oils are described in Table S1.

Three commonly used commercial dispersants, Slickgone NS (Dasic International Ltd., Romsey, Hampshire, UK), Corexit 9500A (Nalco Environmental Solutions LLC, Suger Land, Tx, USA), and Finasol OSR-52 (Total Special Fluids, Paris, France), were included in this study. Slickgone NS is an approved dispersant for several European countries, including use as a secondary tool in oil spill operations on the Norwegian Continental Shelf. Corexit 9500A was injected at the wellhead during the Deepwater Horizon spill in 2010, but also on surfaced oil during the spill (Atlas and Hazen, 2011; Kujawinski et al., 2011). Finasol OSR-52 is a common dispersant approved for use in several countries worldwide.

Natural SW was collected from a depth of 80 m (below thermocline) in a Norwegian fjord (Trondheimsfjord; 63°26'N, 10°23'E), outside the harbour area of Trondheim. The SW is supplied via a pipeline system to our laboratories, and the water source is considered to be non-polluted and not influenced by seasonal variations, with a salinity of 34‰. Inorganic nutrient analyses of the SW showed 130 µg/L nitrite/nitrate, 3 µg/L ammonium and 16 µg/L orto-phosphate (Brakstad et al., 2015a).

2.2 Dispersibility testing

Oil dispersibility was tested with the three dispersants by high energy, according to the Mackay-Nadeau-Steelman (MNS) method (Mackay and Szeto, 1981), generating breaking waves during dispersion. The test system and method has recently been described (Daling et al., 2014). Both fresh oils and w/o emulsions of evaporated (250°C+) or photo-oxidized oils were included (Daling et al., 1990). Fresh oils (0.8 g) or emulsions (8 g emulsion with 50% or

75% (w/w) SW) were applied to 6 L SW, and dispersants applied on the oil surface at dispersant-to-oil ratios (DORs) of 1:100 (fresh oils) or 1:25 (emulsions). The oils and dispersants were allowed to mix for 1-2 minutes. The experiments were performed with continuous breaking wave conditions (generated by blowing air across the SW surface) at 13°C for up to 6 hours. Samples were then collected from the water column at different times during the experiments (5, 15, 30, 60, 130, 240, and 360 minutes) for measurements of oil droplet concentrations and size distributions by Coulter Counter (see below).

Standard dispersibility testing of Troll evaporated or photo-oxidized emulsions (see above) with 50% (w/w) SW were tested with Slickgone NS, Corexit 9500A and Finasol OSR-52 (DOR 1:25) in the MNS system for 120 minutes at 13°C. Dispersant efficiency was determined by UV spectrophotometry (410 nm), and oil droplet concentrations and size distributions by Coulter Counter (see below).

2.3 Interfacial tension (IFT) measurements

IFT measurements were performed in a Spinning Drop Tensiometer (SVT-20N with SVTS 20 control and calculation software DataPhysics Instruments GmbH, Filderstadt, Germany) with a heating/refrigerated circulator for temperature control (F12-ED, Julabo GmbH, Seelbach, Germany). Prior to each measurement the capillary tube was rinsed three times with dichloromethane (DCM) and deionized water, then dried (N_2 gas), and finally rinsed three times with the SW. The capillary was carefully filled with the SW (outer phase liquid) to ensure absence of air bubbles, the open side of the capillary closed with a septum, and the fast exchange capillary inserted into the measuring cell.

Crude oil (10-30 µL), premixed with dispersant (DOR 1:100) or without dispersant, was injected into the stationary capillary tube by a 1 ml syringe with a long needle. Rotation was then immediately started. Rotation speed depended on the IFT of the droplet, ranging from 500-900 r.p.m. (low IFT) to 3000-5000 r.p.m. (high IFT). IFT measurements were initiated immediately after preparation of the droplet in the capillary. During first 5 minutes, IFT was measured after every 5 seconds and after this IFT was recorded after interval of 30 seconds. The measurements were run over night at 13°C but the IFT remains stabilized after 2-4 hours depending upon the type of oil samples.

2.4 Biodegradation experiments

Biodegradation experiments were performed with chemically dispersed oils in natural SW at 13°C for up to 64 days. The SW was not amended with additional mineral nutrients. Fresh oils were premixed with dispersant (DOR 1:100), except the most viscous oil (Grane, see Table S1, Supplementary Information), which required a DOR of 1:50 for efficient dispersibility). An emulsion of Statfjord oil (75 % (w/w) SW content) was pre-mixed at a DOR of 1:25.

Dispersions of fresh oils were prepared in an oil droplet generator, as previously described (Brakstad et al., 2015a; Brakstad et al., 2016; Nordtug et al., 2011). In this system, stock solutions of small oil-droplet dispersions were generated. Stock dispersions were first made with median oil droplet sizes of 10-30 µm and nominal concentrations of 200 mg/L oil in filtered SW (filtered with 1 µm exclusion limit). The droplet concentrations and size distribution were measured by Coulter Counter analyses (see below). The Coulter Counter data were then used to dilute the stock dispersions to final concentrations of 2-3 mg/L in natural SW in glass flasks (2 L; Schott; baked and autoclaved). The flasks were completely filled with the diluted dispersions (no headspace) to avoid any evaporation during the biodegradation period, and sealed with PBT screw caps. Dispersions of oil emulsions were prepared in the MNS-system, as described above. The emulsions of were prepared with 75% (w/w) water from evaporated (200°C+) Statfjord C oil. The dispersions were prepared with Slickgone at a DOR of 1:25. After 2 hours of continuous wave actions, oil droplet concentrations and median droplet sizes in the MNS-system were determined by Coulter Counter analyses, and measured concentrations used to dilute the dispersions to 2-3 mg/L in natural SW, as described above for the oil droplet generator system.

The flasks with diluted dispersions from the oil droplet generator or the MNS-system were mounted on a carousel system, which was slowly rotated around the carousel axis (0.75 r.p.m), to reduce droplet rising (Brakstad et al., 2015a; Brakstad et al., 2016). The flasks were incubated with continuous rotation at 13°C for up to 64 days. Sterilized dispersions were also prepared (100 mg/L $HgCl_2$), in addition to experimental blanks (flasks were filled natural SW without oil). Flasks (triplicate) with dispersions in natural SW, sterilized controls (1-2 replicates) and experimental blanks (1 replicate) were sacrificed for chemical and microbiological analyses after incubation in 0 (15-20 minutes), 3, 7, 14, 21, 28 and 64 days.

2.5 Analyses

2.5.1 Oil droplet analyses

Oil droplet concentrations and size distributions were determined by Coulter Counter measurements (Beckman Multisizer 4; Beckman Coulter Inc., Brea, CA, U.S.A) fitted with 100 µm or 280 µm apertures, for measurement of droplets within a diameter range of 2.0-60 µm or 5.6-100 µm. respectively. Filtered (0.22 µm) SW was used as electrolyte. All droplet sizes reported here are expressed as median droplets diameter on droplet volume if not otherwise mentioned. Particle calibration was verified before analyses by a control samples of Coulter CC Size Standard L10 (aperture 100 µm) or L30 (aperture 280 µm) polystyrene particles (Beckman).

2.5.2 Chemical analyses

Samples of dispersions and SW were solvent-solvent extracted with DCM for measurements of semivolatile organic compounds (SVOC). A gas chromatograph coupled to a flame ionization detector (GC-FID; Agilent 6890N with 30 mDB1 column; Agilent Technologies) was used for quantification of C_{10}-C_{36} total extractable organic carbon (TEOC), and saturates separated by boiling point ranges (C11-C12, C13-C14, C15-C16, C17-C18, C19-C20, C21-C25, C25-C40 [C25+]). *o*-Terphenyl (10 µg/ml) was used as surrogate internal standard (SIS), and 5α-androstane as recovery internal standard (RIS). Targeted analytes were quantified in a gas chromatograph coupled to a mass spectrometer (GC-MS; Agilent 6890 plus GC coupled with an Agilent 5973 MSD detector, operated in Selected Ion Monitoring [SIM] modus; Agilent Technologies). GC-MS analyses included *n*C_{10}-*n*C_{36} alkanes, decalines (C10 saturates), phenols, 2- to 5-ring polycyclic aromatic hydrocarbons (PAH) and 17α(H),21β(H)-Hopane (30ab Hopane), as recently described (Brakstad et al., 2014; Brakstad et al., 2015a). Deuterated SIS-PAH (naphthalene, phenanthrene, chrysene, perylene; 50-250 µg/ml) and RIS-PAH (acenaphthene, fluorene; 100 µg/ml) were included for analyses. The response values for individual target analytes were determined, with a signal-to-noise ratio of 10 as the lower detection limit, and a lower limit of detection (LOD) of 0.01 µg/L was defined for individual oil compounds. Experimental blanks (deionized water) and a QA oil spike (a standard fresh paraffinic oil) were included in analyses of all test batches for GC-FID and GC-MS analyses. In addition, a QA PAH spike was included in all GC-MS test batches.

2.5.3 *Temperature, dissolved oxygen, nutrients, and microbial concentrations*

Air and SW temperatures were measured through the experimental periods and were shown to be within 13±2°C during the experiments (not shown). Dissolved oxygen was measured by a dissolved oxygen meter (YSI, Inc., Yellow Springs, OH) and was never lower than 50 % saturation at the end of the experiments (not shown). Mineral nutrients were not analyzed, but results from previous studies have shown that the oil concentrations used in these studies did not result in mineral nutrient deficiency (Brakstad et al., 2015a).

Microbial cell concentrations were quantified by epifluorescence microcopy analyses of samples stained by the nucleic acid stain 4',6-diamidino-2-phenylindol (Porter and Feig, 1980). Most-probably number (MPN) calculations of heterotrophic prokaryotes (HP) were determined after incubation of dispersions in Marine Broth 2216 at relevant temperature (13°C) for 7 days, while MPN-determinations of oil-degrading prokaryotes (ODP) were performed in SW-based Bushnell-Haas broth by the sheen-screen method (Brown and Braddock, 1990), with 0.1 % (vol/vol) of respective oils as carbon sources at 13°C for 14 days. All dilutions and incubations for MPN-determinations were performed in 24-well tissue culture plates with 2 ml volumes per well. At the end of incubations fluorescein diacetate (FDA) was applied to all wells with Bushnell-Haas medium (0.1 mg/well) and incubated for 60 minutes (room temperature) for observations of metabolic activity (Brown and Braddock, 1990).

2.6 *Calculations and statistics*

Depletion of oil compounds in natural SW and sterilized controls was determined using the ratios between oil target compounds and the recalcitrant biomarker recalcitrant biomarker 17α(H),21β(H)-Hopane (Prince et al., 1994). Biotransformation was then determined by calculating the ratios in natural SW relative to the ratios in sterilized SW to correct for potential abiotic depletion, as previously described (Brakstad et al., 2014).

Non-linear regression analyses were performed by the 1st order rate approach with determination of lag-phases included, using the option "plateau followed by one-phase decay" (GraphPad Prism vs. 6.0; GraphPad Software Inc., La Jolla, CA, U.S.A). Rate coefficients ($k1$) were determined for the decay-period, the plateau period defined the lag-phase, and half-lives were determined from rate coefficients and plateau periods ($t1/2$ = plateau period+

ln(2)/*k*1). Rate data were determined for both single oil components and for 22 oil compound groups described in the Oil-Spill Contingency and Response model OSCAR (Brakstad et al., 2015a; Reed et al., 2001).

Column statistics were performed by one-way Anova analyses in GraphPad Prism.

3. Results and discussions

3.1 Oil dispersibility and droplet characteristics

3.1.1 Dispersibility testing

Since biodegradation of dispersed oil is dependent on droplet size, dispersant efficiencies and oil droplet size distributions were important to determine. Dispersibility testing was therefore performed to determine if well-known commercial dispersants effected the dispersibility efficiencies of crude oils with different physical-chemical properties (paraffinic, naphthenic and asphaltenic oils). Both fresh oils and emulsions from artificially weathered oils were included. A DOR of 1:25 is often used for efficiency testing of dispersants (Venosa et al., 2002). In initial dispersibility tests, we therefore adapted a "standard" DOR of 1:25. Studies in the MNS system at 13°C showed that oil droplet generation of chemically dispersed w/o emulsions (75 % water content) with Slickgone NS (DOR 1:25) required 60 minutes to reach maximum droplet concentrations. The droplet concentrations remained constant for a period of 6 hours with constant wave actions at median oil droplet sizes of 20-25 µm (Fig. 1). Further dispersibility testing of evaporated (250°C+) and photo-oxidized emulsions of Troll oil (50 % water content) was performed with three dispersants (DOR of 1:25), Slickgone NS, Corexit 9500A and Finasol OSR-52 (Table 1). An oil evaporation at 250°C simulate an oil weathering after 2-5 days on the sea (Daling et al., 1990). Photo-oxidation results in generation of polar compounds and has also been shown to transform alkylated PAH compounds (Garrett et al., 1998). The dispersant efficiencies (UV-measurements) of the emulsions were high (90-98 %) in all emulsions. These data verified the high efficiencies of all the dispersants included in the study at a DOR of 1:25. The median oil droplet sizes ranged between 17.8 µm and 30.9 µm. No large effects of weathering methods (evaporation or photo-oxidation) on dispersant efficiencies of droplet sizes were measured for any of the dispersants, although Corexit and OSR-52 generated smaller droplets (17.8-18.8 µm) than Slickgone (28.3-30.9 µm). These droplet sizes are within the ranges expected to be rapidly biodegraded at low temperatures, as previously shown (Brakstad et al., 2015a).

Although standard dispersibility testing is usually performed at a DOR of 1:25, the field application ratios will generally be lower in practice, and laboratory efficiency testing of Corexit 9500 to disperse oil emulsions showed >95 % dispersant efficiency of dispersing oil emulsions at DORs of 1:25 to 1:100 and 85 % at a DOR of 1:250 in the MNS system (Daling et al., 2014). We therefore used a DOR of 1:100 in later experiments with fresh oils, which is within an expected window of efficiency, and more relevant to real field situations than ratios recommended by the producers. Dispersibility testing of the fresh oils with Slickgone NS and Corexit 9500 was performed to determine droplet size distribution, since droplet size is important for biodegradation of dispersed oil (Brakstad et al., 2014, Brakstad et al., 2015a). Average median droplet sizes of 39 ± 6 µm with Slickgone and 30 ± 6 µm with Corexit were measured at a DOR of 1:100 (Fig. S1, Supplementary information). The larger droplet sizes with both dispersants were measured with the asphaltenic Grane oil, which is the most viscous of the oils included here. All oils included in the study were therefore efficiently dispersed with the commercial dispersants included in this study, with oil droplet sizes expected to stimulate oil biodegradation (Brakstad et al., 2015a).

Since Finasol OSR-52 and Corexit 9500A showed similar dispersibility properties, we decided to proceed with only one of these dispersants, Corexit, as well as Slickgone NS, the latter being a preferred dispersant for the Norwegian Continental Shelf.

3.1.2 Changes in oil interfacial tension (IFT)

A Spinning Drop Tensiometer was used to determine oil droplet surface changes as the results of dispersant application. Dispersants are expected to attach to the oil surfaces for generation of the oil-in-water dispersions, but may then leach from the oil surface (Lewis et al., 2010). These changes can be measured by changed IFT. These analyses were performed at 13-20°C with all oils (fresh) included in the study pre-mixed with Slickgone and Corexit. IFTs of the oils not premixed with dispersants were stable at 7-10 mN/m by spinning drop measurements, while dispersant treatment (DOR 1:100 of Slickgone or Corexit) at 20°C resulted in immediate IFT reduction to < 0.01 mM/m of all four oils (not shown).

If temperature was decreased to 13°C, only Troll and Grane oils generated spinning oil droplets possible to measure. Statfjord and Balder oils generated droplets of irregular morphology, and IFT therefore became impossible for these oils at 13°C. Fig. 2 shows the

IFT results over a 4-hour period at 13°C, with Troll and Grane oils premixed with Corexit or Slickgone. For both crude oils, the speed of capillary had no effect on the size of droplet due to reduction in flow characteristics. This is due to the high wax contents of both crude oils which affected their flowability properties. Both dispersants immediately reduced the IFT of the Troll oil to below 0.001 mN/m, but dispersant leaching appeared more rapidly with Slickgone than Corexit (Fig. 2). This may infer that the time-window for generation of small-droplet dispersions may be longer for Corexit than Slickgone. These data also coincided with the generation of larger droplets of Troll oil emulsions by Slickgone than Corexit (Table 1). For the Grane oil, Slickgone did not effectively reduce the oil IFT. However, Corexit was relatively more effective with this oil. IFT reduction of Grane oil with Corexit started after one hour, contrasting the immediate effect measured on the Troll oil (Fig. 2), but resulted in a stable IFT of the Grane oil over the 4 hour testing period. Minimal leaching of active Corexit components were therefore indicated from the surface of the Grane oil. Thus, the two oils with different properties behaved differently with respect to IFT properties. According to a recent study, the increased IFT during dispersant leaching is associated with rapid loss of the surfactant dioctyl sodium sulfosuccinate (DOSS) to the water, and gradually less dispersant adsorption to the oil as the surfactant concentration of Span 80 increased on the oil-SW interface (Riehm and McCormick, 2014).

Comparison of the MNS and the IFT results confirmed differences between Corexit and Slickgone with respect to the effectivity on different oils and time of efficiency. For the napthtenic oil, the two dispersants showed comparable characteristics, but for the more viscous asphaltenic Grane oil, Corexit was more effective than Slickgone, shown both by MNS and IFT testing. Differences in leaching characteristics may also be of importance for selection of dispersants in oil spill operations.

3.2 Biodegradation of dispersed oils

To compare biodegradation in SW of the chemically dispersed oils with different properties, experiments were performed in natural SW, using a carousel system designed to maintain the droplet size distribution in the oil dispersions while incubating the dispersions over time (Brakstad et al., 2015a). All experiments were performed at 13°C over a period of 64 days.

3.2.1 Fate of oil droplets

Chemically prepared dispersions of the oils were generated in the MNS system (Statfjord oil emulsion) or by the oil droplet generator (fresh Statfjord, Troll, Balder and Grane oils), after premixing of oils with dispersant (DOR 1:100) before start of the biodegradation experiments. Although Corexit seemed to be more efficient than Slickgone from the IFT testing (slower leaching time), Slickgone is still an efficient dispersant at the temperature used here See Table 1 and Fig. 1), being the recommended dispersant for the Norwegian Continental Shelf. Slickgone was therefore used to disperse fresh Statfjord, Troll and Balder oils and Statfjord emulsions. However, Corexit was used with the Grane oil, since this dispersant was shown to be more efficient than Slickgone with this oil, as shown by the dispersibility and IFT tests. Corexit also generated Grane oil dispersions with smaller oil droplets, which were easier to keep in suspension, than Slickgone (Fig. S1). The initial median oil droplet concentrations (Table S2) ranged from 2.51 ± 0.18 (Grane) to 2.84 ± 0.03 mg/L (Balder), within the nominal concentrations of 2-3 mg/L. The median oil droplet size distributions (Table S2) were related to the viscosities of the oils (Table S1), ranging from 9.18 ± 0.06 µm for the Statfjord fresh oil (viscosity 12 mPas), to 23.24 ± 2.53 µm for the asphaltenic Grane oil (667 mPas) and 27.95 ± 2.16 µm for the Statfjord emulsion (679 mPas). Increasing viscosity therefore resulted in larger droplet sizes, as shown with the Grane oil and the Statfjord emulsion (See Table S1 and Table S2).

The oil droplets represented surface areas of 2.17 ± 0.05 x 10^6 μm^2/ml for the dispersions with the smallest oil droplets (fresh Statfjord), to 0.87 ± 0.03 x 10^6 μm^2/ml and 0.82 ± 0.01 x 10^6 μm^2/ml for the for the dispersions with the largest oil droplets, Statfjord emulsions and Grane oil, respectively (Table S2). These "large-droplet" dispersions therefore represented only 38 – 40 % of the oil surfaces in the small-droplet Statfjord (fresh) dispersions. A larger surface-to-volume ratio occur with the smaller droplets, resulting in more attachment area for oil-degrading bacteria (Horowitz et al., 1975; Vilcaez et al., 2013).

Changes in oil droplet concentrations during the biodegradation experiments are summarized in Fig. 3, while changes in dispersions of the different oils/emulsions are shown Fig. S2 (Supplementary Information). The oil droplet concentrations were rapidly reduced in all the dispersions, and after 28 days of degradation > 80 % (range 83-98 %) of the droplets in the Coulter Counter measuring range had disappeared from the dispersions (Fig. 3). These reductions were faster in the dispersions of the oils with the initially highest droplet sizes

(Statfjord emulsion and Grane fresh; Fig. S2). Removal of oil droplets may therefore be related to oil droplet rising velocities. The reductions of droplet concentrations also concurred with the emergences of macroscopic 'flocs' (Fig. S3, Supplementary Information), known to consist of oil degradation products, microbes and extracellular polymeric substance (EPS) (Bælum et al., 2012; Hazen et al., 2010). Typically, macroscopic 'flocs' were observed between 1 and 2 weeks of incubation. Oil droplet depletion was also rapid in sterilized dispersions, but slower than in natural SW, and reached 63-95 % depletion after 28 days (Fig. 3 and Fig. S2). Oil droplet size distributions in dispersions with low initial droplet sizes (Statfjord fresh, Troll and Balder) were maintained below 15 µm median droplet size, except Balder and Statfjord fresh, which showed temporary increases to > 20 µm (Fig. S2). Oil dispersions consisting of larger initial droplet sizes (Grane and Statfjord emulsions) also showed decreased droplet sizes (< 20 µm) during the degradation periods (Fig. S2). The fate of the oil droplets was therefore comparable in all dispersions of oils/emulsions with different properties, with rapid declines in droplet concentrations and emergences of 'flocs', while the rest of the free dispersions were dominated by small oil droplets.

The oil droplet depletion, determined by Coulter Counter measurements, was faster than oil depletion determined by TEOC analyses (Fig. 4 and Fig. S4, Supplementary information). In addition to the 'floc' generation processes, glass wall attachments of oil compounds were expected to be a major cause to the droplet depletion in the sterilized samples. The attachments were associated mainly with oleophilic compounds, and in sterilized SW approximately 35 % of *n*-alkanes in the residual oil were extracted from the glass walls at the end of the experiments, while only 7 % naphthalenes and 17 % of 3-ring PAH were attached (Fig. S5, Supplementary Information).

3.3 Biotransformation of TEOC and targeted compounds

Biodegradation of TEOC and targeted compounds (nC_{10}-nC_{36} alkanes and 2- to 4-ring PAH) were determined by normalizing target analyte concentrations against the recalcitrant biomarker 17α(H),21β(H)-Hopane (Prince et al., 1994), and then correcting for depletion in sterilized controls. The average results of TEOC, *n*-alkanes and PAH of the oils and the emulsion are summarized in Fig. 4, while biotransformation curves of each oil/emulsion are shown in Fig. S6 (Supplementary Information). The biotransformation of TEOC, *n*-alkanes and PAH showed comparable results for all the dispersed oils and the emulsion. However, the

dispersions of the most viscous oils (Grane oil and Statfjord emulsion), with the largest initial median oil droplet sizes (Table S2), showed slightly slower TEOC depletion than the other oils (Fig. S6, Supporting Information). TEOC was degraded by > 70 % in all dispersions (average 75.0 ± 7.5 %) at the end of the experiments (Fig. 4). *n*-Alkanes were biotransformed by > 90 % in all dispersions after 14 days (average 96.6 ± 2.7 %), ranging from 92.2 to 99.2 % (Fig. 4 and Fig. S6). PAHs were also biotransformed fast, being depleted by > 80 % after 14 days (average 86.0 ± 4.6 %, range 81.5 to 92.2 %) (Fig. 4 and Fig. S6). Closer examination of targeted compounds showed decreased *n*-alkane biotransformation by increased carbon chain-length, but after 14 days of incubation, all *n*-alkanes in the dispersions were transformed by > 80 % (Fig. S7A, Supplementary Information). Even the isoprenoids (Pristane and Phytane) were highly biotransformed in the dispersions, with Pristane averaging 90.3 ± 9.8 % and Phytane 83.8 ± 15.3 %. Biotransformation of the *n*-alkanes in the Statfjord emulsion started earlier than in the fresh oils, but after 14 days the *n*-alkanes in the emulsion were less depleted than the other oils (Fig. S7A). Biotransformation of PAH compounds decreased correspondingly by increased aromatic ring numbers, but also by increased alkyl substitutions (Fig. S7B, Supplementary Information), as previously shown (Brakstad et al., 2014; Brakstad et al., 2015a). All 2- to 3-ring PAHs were completely biotransformed in dispersions from fresh oils after 28 days of biodegradation, and ≥88 % in the dispersions from the emulsion. Biotransformation of 4-ring PAHs continued from 28 to 64 days, and only C3-alkylated fluoranthenes/pyrenes C2-alkylated chrysenes remained in the dispersions from fresh oil (77-85 % biotransformation). The remaining PAH in the dispersed emulsions after 64 days included alkylated phenanthrenes, dibenzothiophenes, fluoranthenes/pyrenes and chrysenes (30.2 to 96.5 % biotransformed). The biotransformation of targeted *n*-alkane and PAH compounds in the dispersions resulted in an increase of the unresolved fraction of the oil, as measured by GC-FID. This fraction, termed the "unresolved complex mixture" (UCM), increased from 78-88 % in the initial dispersions with paraffinic oils content (Statfjord and Balder blend), and 94-97 % in the asphaltenic Grane and naphthenic Troll oils, to 99-100 % after 28 days of incubation (Fig. S8, Supplementary Information). The UCM fractions thus became completely predominant during the biodegradation period.

Ranges of half-lives for targeted oil compounds, determined from 1st order rate coefficients, varied from 1.7 to 11.7 days for *n*-alkanes, with average values for the oils ranging from 2 to 6 day with increasing chain length (Fig. 5A). For 2- to 4-ring PAH half-lives varied from 3.6 to 80 days, with average values ranging from 5 to 30 days (Fig 5B). One-way Anova analyses did not show significant differences between TEOC or PAH

biotransformation in the different dispersions (P>0.05), while *n*-alkane transformation showed significant differences (P<0.05). The *n*-alkane differences were caused by lower half-lives for the Statfjord emulsion, probably related to the higher initial median oil droplet size of emulsion compared to the fresh oils (Table S2, Supporting Information). However, *n*-alkane degradation was fast also in the emulsion. Comparison of the dispersions from the fresh oils only (excluding the emulsion) resulted in comparable *n*-alkane half-lives (P>0.05). Differences in biotransformation were therefore not determined between the fresh oils with different properties. We have recently observed that *n*-alkanes, associated with the oil phase, are more dependent on initial droplet size than the aromatic hydrocarbons (Brakstad et al., 2014), indicating that the aromatics to a greater extent are degraded after dissolution to the water phase. The ranges of *n*-alkane and PAH half-lives of the oils in the current experiments were lower than for biodegradation at 5°C of chemically dispersed Macondo oil in SW from the Trondheimsfjord or GoM (Brakstad et al., 2015a; Wang et al., 2016), and also from estimated half-lives of the DWH deepwater plume (Hazen et al., 2010). This was expected as the incubation temperatures were higher in the current experiments (13°C). However, even shorter half-lives than in our experiments were measured for several oil compounds when chemically dispersed oil was biodegraded in New Jersey SW at 8°C incubation temperature (Prince et al., 2013), suggesting that SW sources affect degradation rates.

3.4 Biotransformation of oil compound groups

We have previously described biotransformation rates of 22 oil compound groups, separated in 10 volatile and 12 semivolatile groups (Brakstad and Faksness, 2000; Brakstad et al., 2015a). The grouping is based on separation according to boiling point ranges, covering 70-80 % of typical crude oils (Pasquini and Bueno, 2007). Transformation rates for each of these groups have been included in the three-dimensional dynamic OSCAR model as part of the fate calculations of oil spills to the marine environment (Reed et al., 2001). In this study we only included comparison of semivolatile groups, since most of the volatiles were evaporated in the emulsion. Biotransformation half-lives for the semivolatile groups ranged between 7 and 67 days for saturates, increasing by higher boiling point ranges (Fig. 6). The average values for the oil saturates included in the study increased from 9 to 47 days by increasing boiling point range. These saturates, as determined by GC-FID analyses, included both *n*-alkanes and the unresolved part (UCM) of each boiling point range in the GC-FID chromatograms. The *n*-alkanes were degraded faster than the UCM (Fig. S8), but also the

UCM half-lives were related to boiling point range, as shown in Fig. 6. Biotransformation half-lives of naphthalenes and 2- to 5-ring PAHs ranged between 3 and 24 days, with average half-lives between 5 and 19 days (Fig. 6). One-way ANOVA comparison of half-lives for each of the oils did not show significant differences ($P>0.05$). The data from the current study confirmed that degradation data were comparable between oils with different physical-chemical properties in small-droplet oil dispersion. Our data are in support of using generic rather than oil-specific data as part of fate-prediction after dispersant treatment of oil spills at environmentally conditions comparable to those used in this study. The data generated here are more robust than results from previous studies with only paraffinic oils (Brakstad and Faksness, 2000; Brakstad et al., 2015a). Recent studies with chemically dispersed Macondo oil in natural SW (10 and 30 µm initial oil droplet size) at 5°C incubation temperature showed generally higher half-lives of the same oil compound groups than in the current experiments, probably due to the lower incubation temperature used with the Macondo oil (Brakstad et al., 2015a). Different SW temperatures may both influence the community structures of oil-degrading microbes and the physical-chemical properties of the oils. For instance, low SW temperature may result in increased oil viscosity, reducing biodegradation (Atlas, 1991).

3.5 Stimulation of microbial growth

Microbial concentrations determined by fluorescence microscopy or MPN counts showed rapid growth stimulation in all experiments (Fig. 7 and Fig S9, Supporting In formation). Stimulation of both total concentrations, heterotrophs and oil-degraders appeared mainly during the first week of all experiments, and high concentrations were maintained during the next week (up to day 14), with subsequent slow decline of concentrations between days 14 and 21. The microbial stimulation coincided well with hydrocarbon biotransformation, with > 80 % *n*-alkane and PAH biotransformation after 7 and 14 days, respectively (Fig. 4 and Fig. S6). Subsequent increases of total and heterotrophic concentrations between days 21 and 28 could be the result of available metabolites from hydrocarbon degradation, in agreement with the lack of further stimulation of oil-degrading microbes (Fig. 7). We have previously observed this pattern of two separate microbial stimulation periods during biodegradation of chemically dispersed oil (Brakstad et al., 2015b), and the first stimulation period was associated with microbes with high abundances of the *alkB* gene (Brakstad et al., 2014), involved in alkane biotransformation (van Beilen and Funhoff, 2007).

3 Conclusions

In this study we investigated dispersibilities and biodegradation of chemically dispersed oils and emulsions with different properties at a SW temperature of 13°C, relevant for North Sea and Norwegian Sea summer conditions. The oils, representing paraffinic, naphthenic and asphaltenic oils, were all dispersible at the SW temperature used with the three common commercial dispersants Slickgone NS, Corexit 9500A and Finasol OSR-52, showing median oil droplet sizes of 18-47 µm. However, oils and dispersants behaved differently with respect to IFT reductions and leaching properties at this temperature. Biodegradation was comparable between the oil dispersions in natural SW at low oil concentrations, and the degradation resulted in reduced oil droplet concentrations, coinciding with the generation of 'flocs', probably consisting of oil, bacteria and polymeric material. Oil properties affected dispersibility only slightly. The most viscous oil and the emulsion resulted in dispersions with the highest median droplet sizes. The results showed that the selected oils and emulsions were efficiently dispersed to generate small droplets of similar sizes. The oil compound were further biodegraded with comparable biotransformation half-lives in SW at 13°C, despite the differences between the oils. Generic biodegradation data may therefore be considered when models like OSCAR are used to predict the fate of oil after efficient dispersant treatment of oil spills in SW close to 13°C. Using empirical data in the model will strengthen the predictions of the fate of the oil after oil spill dispersant treatment.

Acknowledgements

This study was supported by the Norwegian Research Council Petromaks2 program (contract #228271-E30) and the oil companies Statoil Petroleum AS, ExxonMobil Exploration and Production Norway AS, AkerBP ASA, TOTAL E&P Norge ASA, and ConocoPhillips Skandinavia AS. We will thank Thor-Arne Pettersen, Inger Steinsvik, Marianne Unaas Rønsberg and Inger K. Almås, Marianne Aas, Marianne A. Molid, Bror Johansen, and Daniel F. Krause for chemical analyses and technical assistance.

References

Atlas, R.M. 1991. Microbial hydrocarbon degradation—bioremediation of oil spills. J. Chem. Technol. Biotechnol. 52, 149-156.

Atlas, R.M., Hazen, T.C., 2011. Oil Biodegradation and Bioremediation: A Tale of the Two Worst Spills in U.S. History. Environ. Sci. Technol. 45, 6709-6715.

Brakstad, O.G., Daling, P.S., Faksness, L.-G., Almås, I.K., Vang, S.-H., Syslak, L., Leirvik, F., 2014. Depletion and biodegradation of hydrocarbons in dispersions and emulsions of the Macondo 252 oil generated in an oil-on-seawater mesocosm flume basin. Mar. Pollut. Bull. 84, 125-134.

Brakstad, O.G., Faksness, L.G., 2000. Biodegradation of Water-Accommodated Fractions and Dispersed Oil in the Seawater Column. Proceedings od the SPE International Conference on Health, Safety, and the Environment in Oil and Gas Exploration and Production, Stavanger, Norway, 26–28 June 2000, Paper no. 61466.

Brakstad, O.G., Nordtug, T., Throne-Holst, M., 2015a. Biodegradation of dispersed Macondo oil in seawater at low temperature and different oil droplet sizes. Mar. Pollut. Bull. 93, 144-152.

Brakstad, O.G., Throne-Holst, M., Netzer, R., Stoeckel, D.M., Atlas, R.M., 2015b. Microbial communities related to biodegradation of dispersed Macondo oil at low seawater temperature with Norwegian coastal seawater. Microb. Biotechnol. 8, 989-998.

Brakstad, O. G., Throne-Holst, M., Nordtug, T., 2016. Oil Droplet Generation and Incubation for Biodegradation Studies of Dispersed Oil. In McGenity, T.J., Timmis, K.N., Nogales, B. (Eds.) Hydrocarbon and Lipid Microbiology Protocols, Springer, Berlin, Heidelberg, pp. 237-253.

Brown, E.J., Braddock, J.F., 1990. Sheen screen, a miniaturized most-probable-number method for enumeration of oil-degrading microorganisms. Appl. Environ. Microbiol. 56, 3895-3896.

Bælum, J., Borglin, S., Chakraborty, R., Fortney, J.L., Lamendella, R., Mason, O.U., Auer, M., Zemla, M., Bill, M., Conrad, M.E., Malfatti, S.A., Tringe, S.G., Holman, H.-Y., Hazen, T.C., Jansson, J.K., 2012. Deep-sea bacteria enriched by oil and dispersant from the Deepwater Horizon spill. Environ. Microbiol. 14, 2405-2416.

Campo, P., Venosa, A.D., Suidan, M.T., 2013. Biodegradability of Corexit 9500 and Dispersed South Louisiana Crude Oil at 5 and 25 °C. Environ. Sci. Technol. 47, 1960-1967.

Daling, P.S., Brandvik, P.J., Mackay, D., Johansen, O., 1990. Characterization of crude oils for environmental purposes. Oil Chem. Pollut. 7, 199-224.

Daling, P.S., Leirvik, F., Almås, I.K., Brandvik, P.J., Hansen, B.H., Lewis, A., Reed, M., 2014. Surface weathering and dispersibility of MC252 crude oil. Mar. Pollut. Bull. 87, 300-310.

Garrett, R. M., Pickering, I. J., Haith, C. E., Prince, R. C., 1998. Photooxidation of crude oils. Environ. Sci. Technol., 32, 3719-3723.

Hazen, T.C., Dubinsky, E.A., DeSantis, T.Z., Andersen, G.L., Piceno, Y.M., Singh, N., Jansson, J.K., Probst, A., Borglin, S.E., Fortney, J.L., Stringfellow, W.T., Bill, M., Conrad, M.E., Tom, L.M., Chavarria, K.L., Alusi, T.R., Lamendella, R., Joyner, D.C., Spier, C., Baelum, J., Auer, M., Zemla, M.L., Chakraborty, R., Sonnenthal, E.L., D'haeseleer, P., Holman, H.-Y.N., Osman, S., Lu, Z., Van Nostrand, J.D., Deng, Y., Zhou, J., Mason, O.U., 2010. Deep-Sea Oil Plume Enriches Indigenous Oil-Degrading Bacteria. Science 330, 204-208.

Horowitz, A., Gutnick, D., Rosenberg. E., 1975. Sequential growth of bacteria on crude oil. Appl. Microbiol. 30, 10–19.

Kleindienst, S., Seidel, M., Ziervogel, K., Grim, S., Loftis, K., Harrison, S., Malkin, S.Y., Perkins, M.J., Field, J., Sogin, M.L., Dittmar, T., Passow, U., Medeiros, P.M., Joye, S.B., 2015. Chemical dispersants can suppress the activity of natural oil-degrading microorganisms. PNAS 112, 14900-14905.

Kujawinski, E.B., Kido Soule, M.C., Valentine, D.L., Boysen, A.K., Longnecker, K., Redmond, M.C., 2011. Fate of Dispersants Associated with the Deepwater Horizon Oil Spill. Environ. Sci. Technol. 45, 1298-1306.

Lee, K., Nedwed, T., Prince, R.C., Palandro, D., 2013. Lab tests on the biodegradation of chemically dispersed oil should consider the rapid dilution that occurs at sea. Mar. Pollut. Bull. 73, 314-318.

Lessard, R.R., DeMarco, G., 2000. The Significance of Oil Spill Dispersants. Spill Sci. Technol. Bull. 6, 59-68.

Lewis, A., Ken Trudel, B., Belore, R.C., Mullin, J.V., 2010. Large-scale dispersant leaching and effectiveness experiments with oils on calm water. Mar. Pollut. Bull. 60, 244-254.

Lindstrom, J.E., Braddock, J.F., 2002. Biodegradation of petroleum hydrocarbons at low temperature in the presence of the dispersant Corexit 9500. Mar. Pollut. Bull. 44, 739-747.

Mackay, D., Szeto, F., 1981. The laborattory determination of dispersant effectiveness: Method development and results. International Oil Spill Conference Proceedings 1981, 11-17.

Macnaughton, S.J., Swannell, R., Daniel, F., Bristow, L., 2003. Biodegradation of Dispersed Forties Crude and Alaskan North Slope Oils in Microcosms Under Simulated Marine Conditions. Spill Sci. Technol. Bull. 8, 179-186.

McFarlin, K.M., Prince, R.C., Perkins, R., Leigh, M.B., 2014. Biodegradation of dispersed oil in arctic seawater at-1 C. PloS one 9, e84297.

Nordtug, T., Olsen, A.J., Altin, D., Meier, S., Overrein, I., Hansen, B.H., Johansen, Ø., 2011. Method for generating parameterized ecotoxicity data of dispersed oil for use in environmental modelling. Mar. Pollut. Bull. 62, 2106-2113.

Pasquini, C., Bueno, A.F., 2007. Characterization of petroleum using near-infrared spectroscopy: Quantitative modeling for the true boiling point curve and specific gravity. Fuel 86, 1927-1934.

Porter, K., Feig, Y., 1980. The use of DAPI for identification and enumeration of aquatic microflora. Limnol. Oceanogr. 25, 943-947.

Prince, R.C., 2015. Oil Spill Dispersants: Boon or Bane? Environ. Sci. Technol. 49, 6376-6384.

Prince, R.C., Elmendorf, D.L., Lute, J.R., Hsu, C.S., Haith, C.E., Senius, J.D., Dechert, G.J., Douglas, G.S., Butler, E.L., 1994. 17.alpha.(H)-21.beta.(H)-hopane as a conserved internal marker for estimating the biodegradation of crude oil. Environ. Sci. Technol. 28, 142-145.

Prince, R.C., McFarlin, K.M., Butler, J.D., Febbo, E.J., Wang, F.C.Y., Nedwed, T.J., 2013. The primary biodegradation of dispersed crude oil in the sea. Chemosphere 90, 521-526.

Rahsepar, S., Smit, M.P.J., Murk, A.J., Rijnaarts, H.H.M., Langenhoff, A.A.M., 2016. Chemical dispersants: Oil biodegradation friend or foe? Mar. Pollut. Bull. 108, 113-119.

Reed, M., Aamo, O.M., Daling, P.S., 1995. Quantitative analysis of alternate oil spill response strategies using OSCAR. Spill Sc. Technol. Bull. 2, 67-74.

Reed, M., Singsaas, I., Daling, P.S., Faksnes, L.-G., Brakstad, O.G., Hetland, B.A., Hofatad, J.N., 2001. Modeling the water-accommodated fraction in OSCAR2000. Proceedings of the International Oil Spill Conference Proceedings 2001, 1083-1091.

Riehm, D.A., McCormick, A.V., 2014. The role of dispersants' dynamic interfacial tension in effective crude oil spill dispersion. Mar. Pollut. Bull. 84, 155-163.

Siron, R., Pelletier, É., Brochu, C., 1995. Environmental factors influencing the biodegradation of petroleum hydrocarbons in cold seawater. Arch. Environ. Contam. Toxicol. 28, 406-416.

Strøm-Kristiansen, T., Lewis, A., Daling, P.S., Hokstad, J.N., Singsaas, I., 1997. Weathering and dispersion of naphthenic, asphalteninc, and waxy crude oils. International Oil Spill Conference Proceedings 1997, 631-636.

van Beilen, J.B., Funhoff, E.G., 2007. Alkane hydroxylases involved in microbial alkane degradation. Appl. Microbiol. Biotechnol. 74, 13-21.

Venosa, A.D., Holder, E.L., 2007. Biodegradability of dispersed crude oil at two different temperatures. Mar. Pollut. Bull. 54, 545-553.

Venosa, A.D., King, D.W., Sorial, G.A., 2002. The Baffled Flask Test for Dispersant Effectiveness: A Round Robin Evaluation of Reproducibility and Repeatability. Spill Sci. Technol. Bull. 7, 299-308.

689 Vilcáez, J., Li, L., Hubbard, S. S., 2013. A new model for the biodegradation kinetics of oil
690 droplets: application to the Deepwater Horizon oil spill in the Gulf of Mexico. Geochem.
691 Transact. 14, 4.
692
693 Wang, J., Sandoval, K., Ding, Y., Stoeckel, D., Minard-Smith, A., Andersen, G., Dubinsky,
694 E.A., Atlas, R., Gardinali, P., 2016. Biodegradation of dispersed Macondo crude oil by
695 indigenous Gulf of Mexico microbial communities. Sci. Tot. Environ. 557–558, 453-468.
696
697 Zahed, M.A., Aziz, H.A., Isa, M.H., Mohajeri, L., 2010. Effect of Initial Oil Concentration
698 and Dispersant on Crude Oil Biodegradation in Contaminated Seawater. Bull. Environ.
699 Contam. Toxicol. 84, 438-442.
700
701 Zahed, M.A., Aziz, H.A., Isa, M.H., Mohajeri, L., Mohajeri, S., Kutty, S.R.M., 2011. Kinetic
702 modeling and half life study on bioremediation of crude oil dispersed by Corexit 9500. J.
703 Hazard. Mat. 185, 1027-1031.
704

TABLES AND FIGURES

Table 1. Dispersant efficiency (UV-measurements) and median oil droplet sizes of emulsions (50 volume % water) of evaporated (250°C+) or photo-oxidized Troll oil dispersed by three dispersants at 13°C.

Dispersant	Weathering	Dispersant efficiency (%)	Median droplet size (µm)
Slickgone NS	250°C+	92	30.9
	Photo-oxidized	90	28.3
Corexit 9500A	250°C+	93	19.8
	Photo-oxidized	90	19.0
Finasol OSR-52	250°C+	93	18.8
	Photo-oxidized	98	17.8

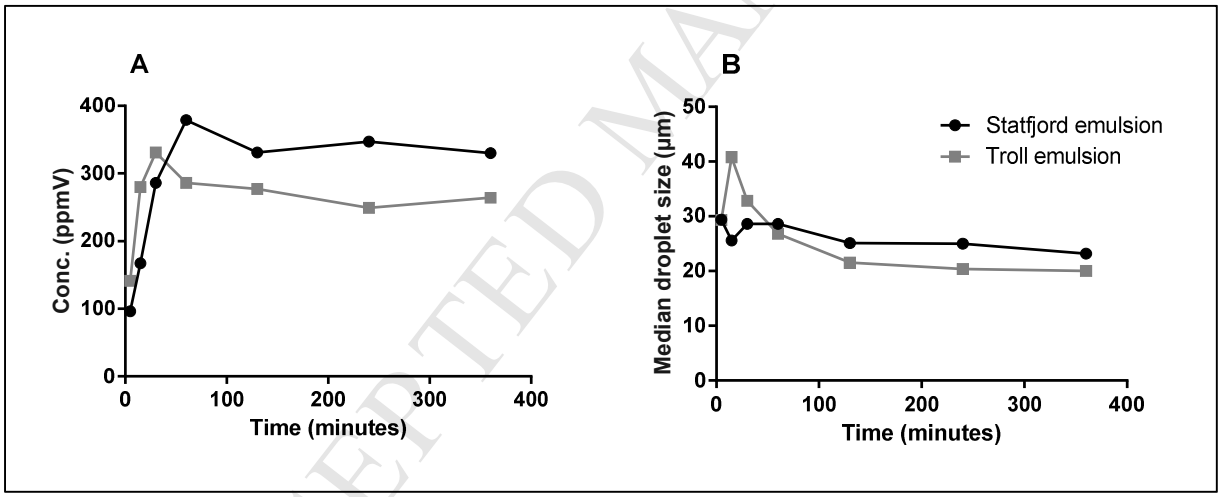

Fig. 1. Concentrations (A) and median oil droplet sizes (B) of Statfjord and Troll emulsions (75 vol % water), dispersed with Slickgone NS (DOR 1:25) over a period of 6 hours.

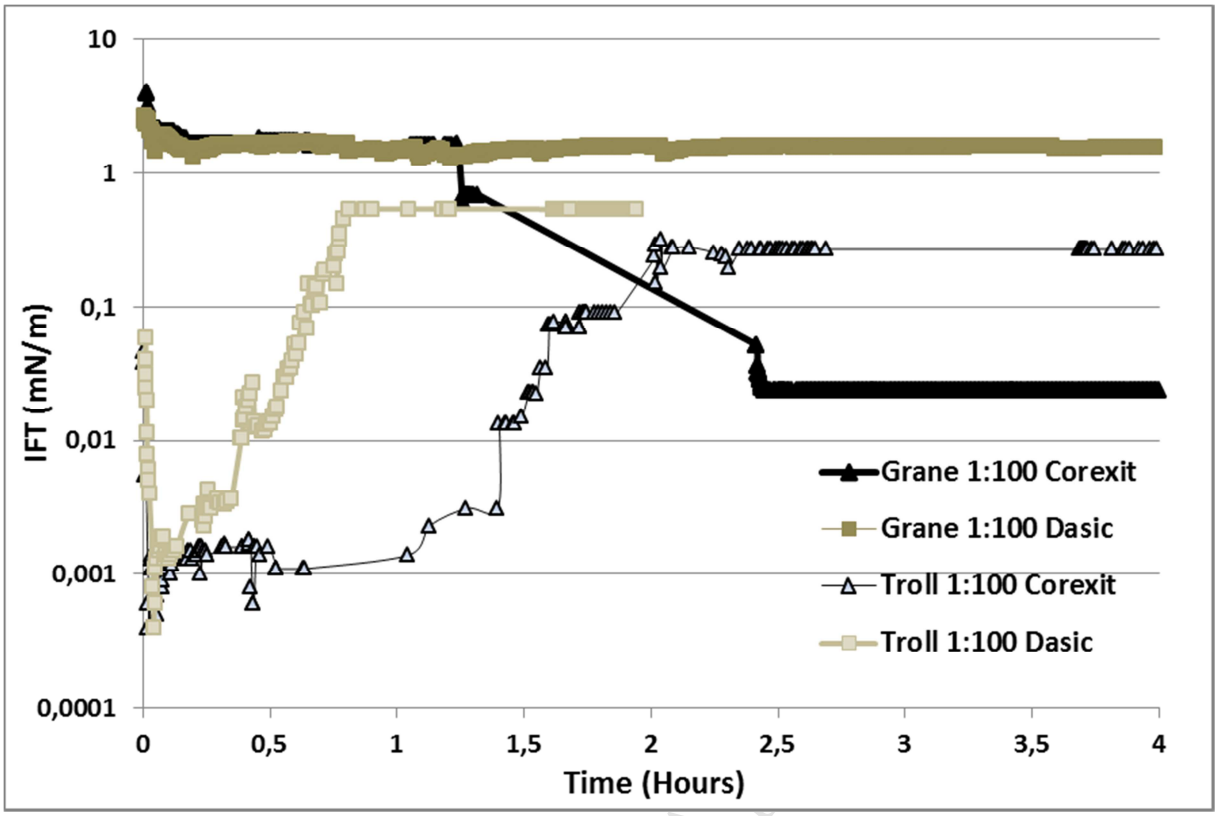

Fig. 2. IFT measurements of naphthenic Troll and asphaltenic Grane crude oils at 13°C after premixing of the oils with the dispersants Corexit 9500 or Slickgone (Dasic) NS in SW (DOR 1:100). Analyses were performed overnight, with results shown for the first 4 hours.

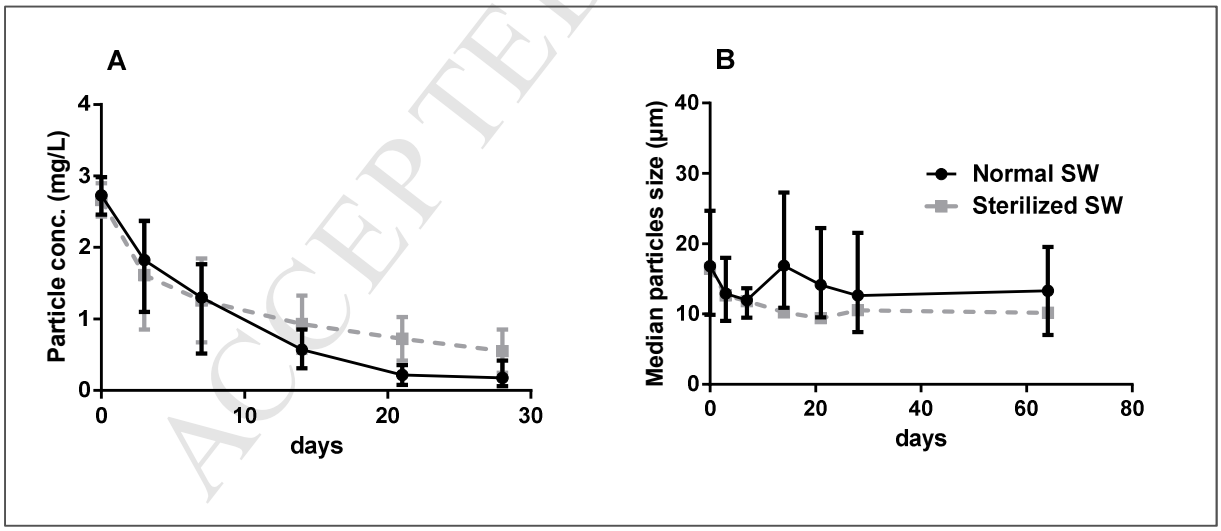

Fig. 3. Oil droplet concentrations (A) and median droplet size distributions (B) in dispersions of fresh oils and emulsions prepared in natural or sterilized SW. The error bars represent the ranges of the measurements (see Fig. S2). The concentrations are shown for the first 28 days of the experiment, and droplet size distribution for all samples.

733

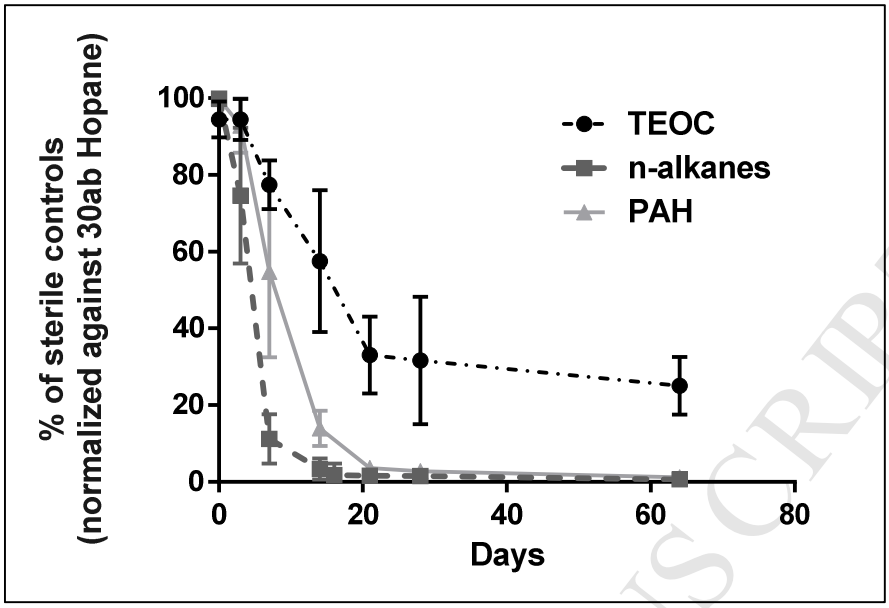

734

735 Fig. 4. Average biotransformation of TEOC, Σn-alkanes (nC$_{10}$-nC$_{36}$) and Σ2- to 4-ring PAH in
736 chemically dispersed oils with different properties, and in a dispersed emulsion, during a
737 period of 64 days in SW at 13°C. Concentrations of *n*-alkanes and PAH were normalized
738 against 17α(H),21β(H)-Hopane (30ab Hopane) and results shown as % of normalized
739 concentrations in sterilized controls from same sampling days. Biotransformation curves of
740 individual oils are shown in Fig. S6 (Supporting Information).

741

742

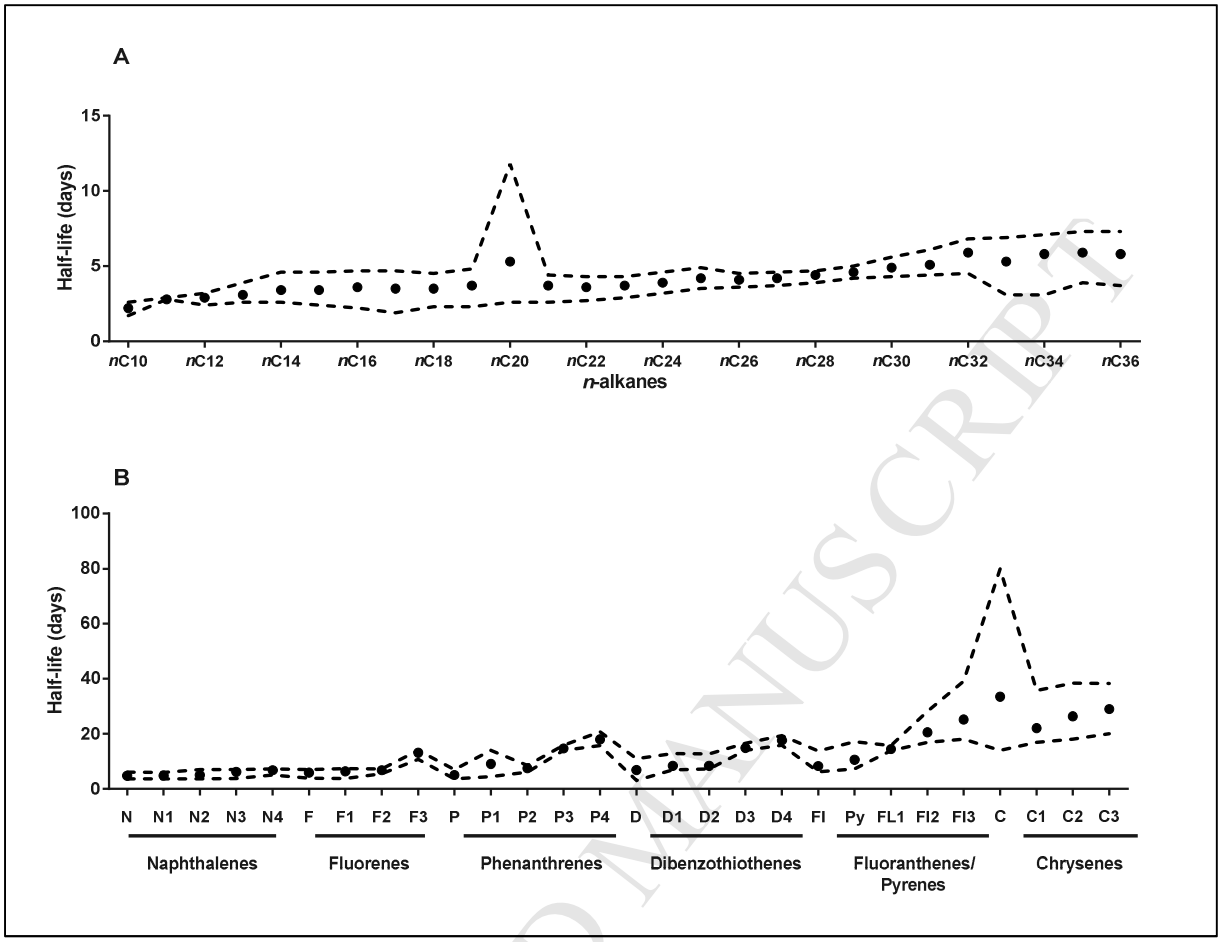

743

744 Fig. 5. Biotransformation half-lives of single nC_{10}-nC_{36} alkanes (A) and of 2- to 4-ring
745 aromatic hydrocarbons (HCs) of different alkyl-substitution (B). The half-lives were
746 determined from 1st order rate coefficients, and corrected for a non-responsive lag-period. The
747 bullets show average values of each compound for all oils included in the study, with dashed
748 lines representing lower and higher ranges.

749

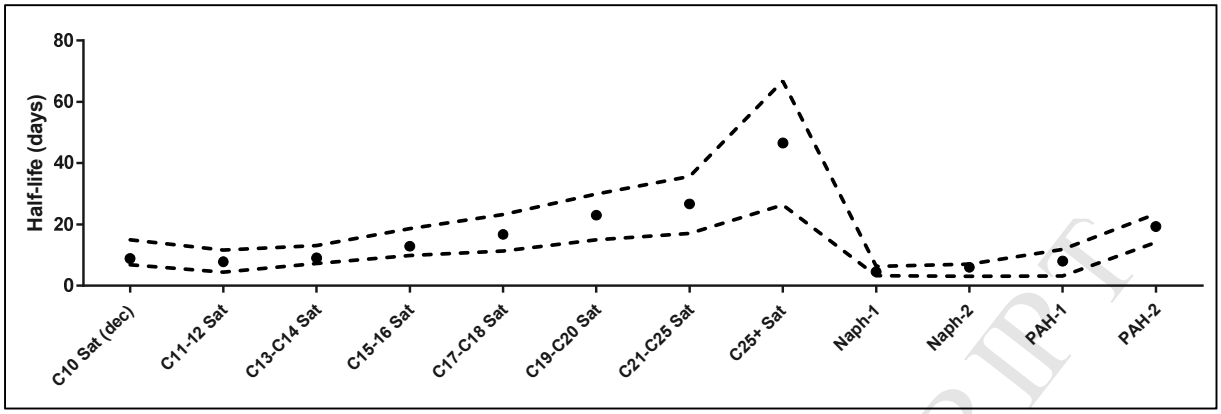

Fig. 6. Half-lives of semivolatile saturate and aromatic groups of the oils included in the study. The half-lives were determined from 1st order rate coefficients, and also includes the non-responsive lag-period. The groups included represent C10-C26 saturates and 2- to 5-ring aromatic HCs. The bullets show average values of each groups, with dashed lines representing lower and higher ranges.

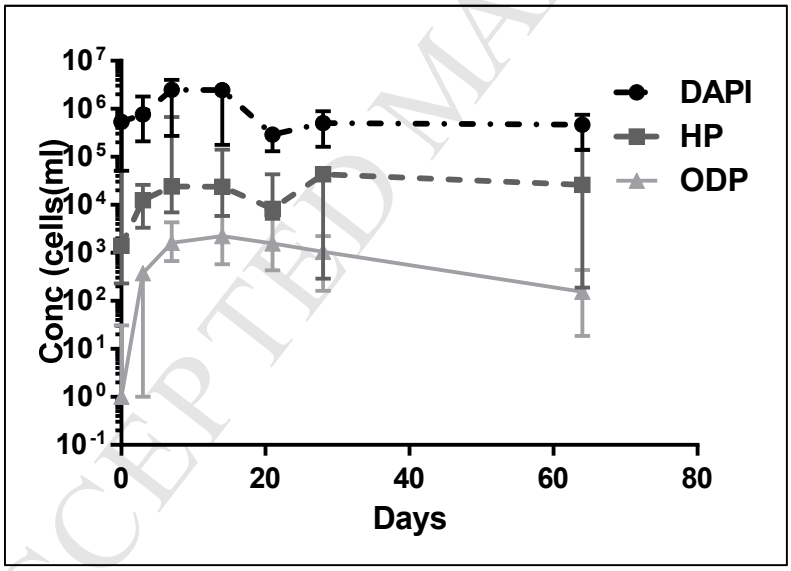

Fig. 7. Concentrations of total microbes counted by fluorescence microscopy (DAPI), heterotrophic prokaryotes (HP), and oil-degrading prokaryotes (ODP). The results are shown as median concentrations with range compiled from the included experiments, based on data with separate oils (see Fig. S9, Supporting Information).

Supplementary Information

Table S1. Physical and chemical properties of crude oils included in this study.

Oil	Category	Viscosity (mPas;13°C)[A)]	Density (g/cm^3)	Pour point (°C)	Wax (vol %)	Asphaltene (wt %)
Statfjord (fr)	Paraffinic	12	0.834	-9	4.1	0.16
Statfjord (200°C+)[B)]	Paraffinic	679	0.883	21	5.8	0.23
Troll C (fr)	Naphthenic	27	0.900	-18	2.0	0.2
Troll C (250°C+)[B)]	Naphthenic	200	0.919	3	2.6	0.2
Troll C (photo-ox.)[B)]	Naphthenic	262	0.924	6	2.3	0.6
Grane	Asphaltenic	667	0.941	-18	1.5	1.4
"Balder"	Mixture[C)]	32	0.864	3	3.5	0.77

[A)] Shear rate of 100 s^{-1}

[B)] Evaporated at 200°C to simulate 0.5-1 day at sea, while 250°C and photo-oxidized simulate 2-5 days at sea (Daling et al., 1990)

[C)] The oil was a blend of 40% asphaltenic Balder and 60% paraffinic Ringhorne oils

Table S2. Droplet characteristics of the oil dispersions at the start of the biodegradation experiments.

Oil	Droplet size (median; µm)	Droplet concentrations (mg/L)	Droplet area (µm^2/mL)	No. droplets/mL
Statfjord C (fr)	9.18 ± 0.06	2.73 ± 0.06	2.17 ± 0.05 x 10^6	10.72 ± 0.26 x 10^3
Statfjord C (em)	27.95 ± 2.16	2.71 ± 0.18	0.87 ± 0.03 x 10^6	1.79 ± 0.08 x 10^3
Troll C	13.36 ± 0.07	2.71 ± 0.09	1.49 ± 0.06 x 10^6	4.72 ± 0.17 x 10^3
Grane	23.24 ± 2.53	2.51 ± 0.18	0.82 ± 0.01 x 10^6	1.44 ± 0.17 x 10^3
"Balder"	12.67 ± 0.69	2.84 ± 0.03	1.71 ± 0.02 x 10^6	5.90 ± 0.12 x 10^3

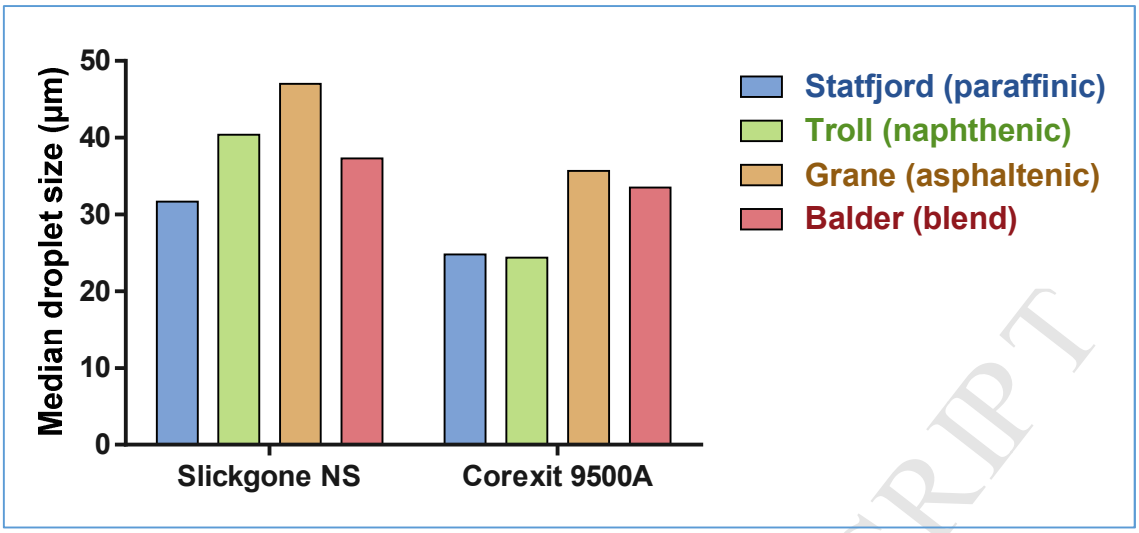

783

784 Fig S1. Median droplet size distributions of fresh oils premixed with Slickgone NS or Corexit
785 9500A (DOR 1:100). Samples used in these analyses were collected after 25 minutes.
786
787

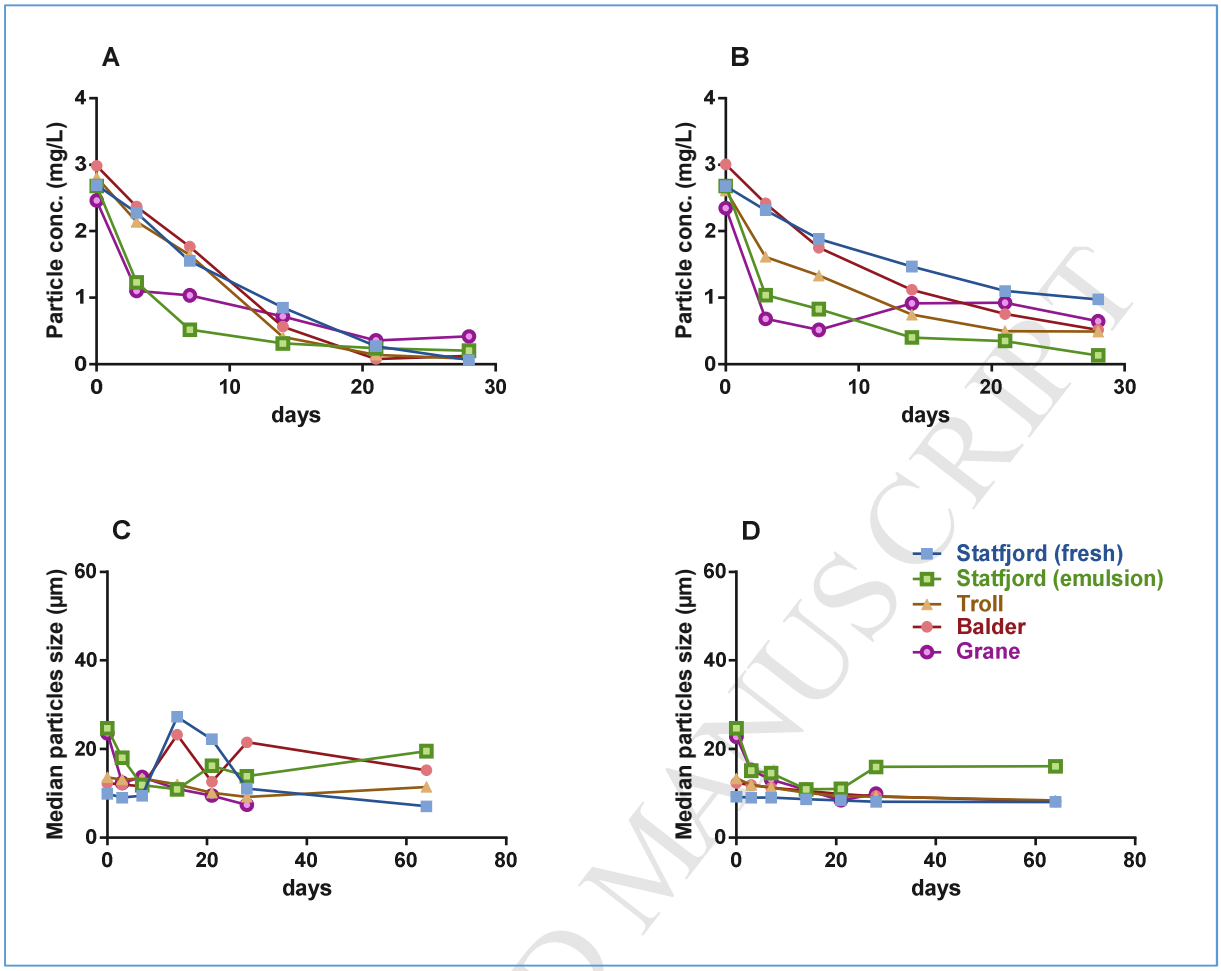

Fig. S2. Oil droplet concentrations in natural (A) and sterilized SW (B), and median droplet size distributions in natural (C) and sterilized (D) SW. The concentrations are shown for the first 28 days of the experiment, while the droplet size distribution is shown for the complete degradation period.

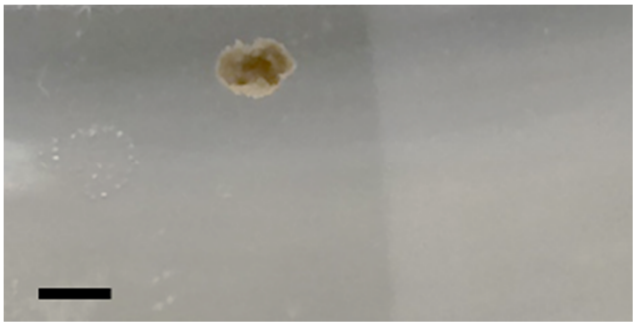

Fig. S3. A typical macroscopic 'floc' observed during oil biodegradation. The scale is 3 mm.

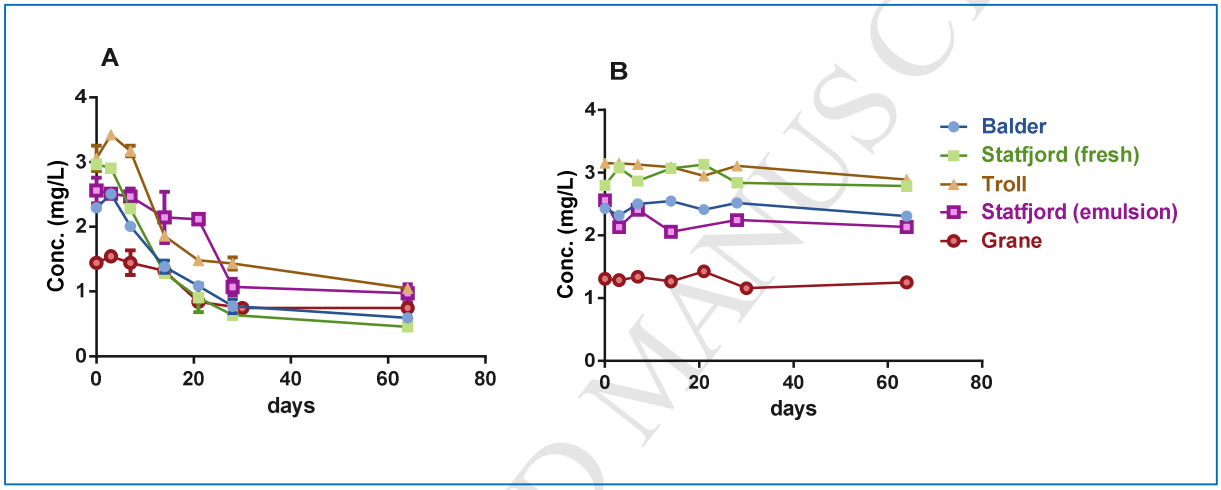

Fig. S4. Concentrations of total extractable organic carbon (TEOC) in dispersions of fresh oils and emulsions prepared in natural (A) and sterilized (B) SW.

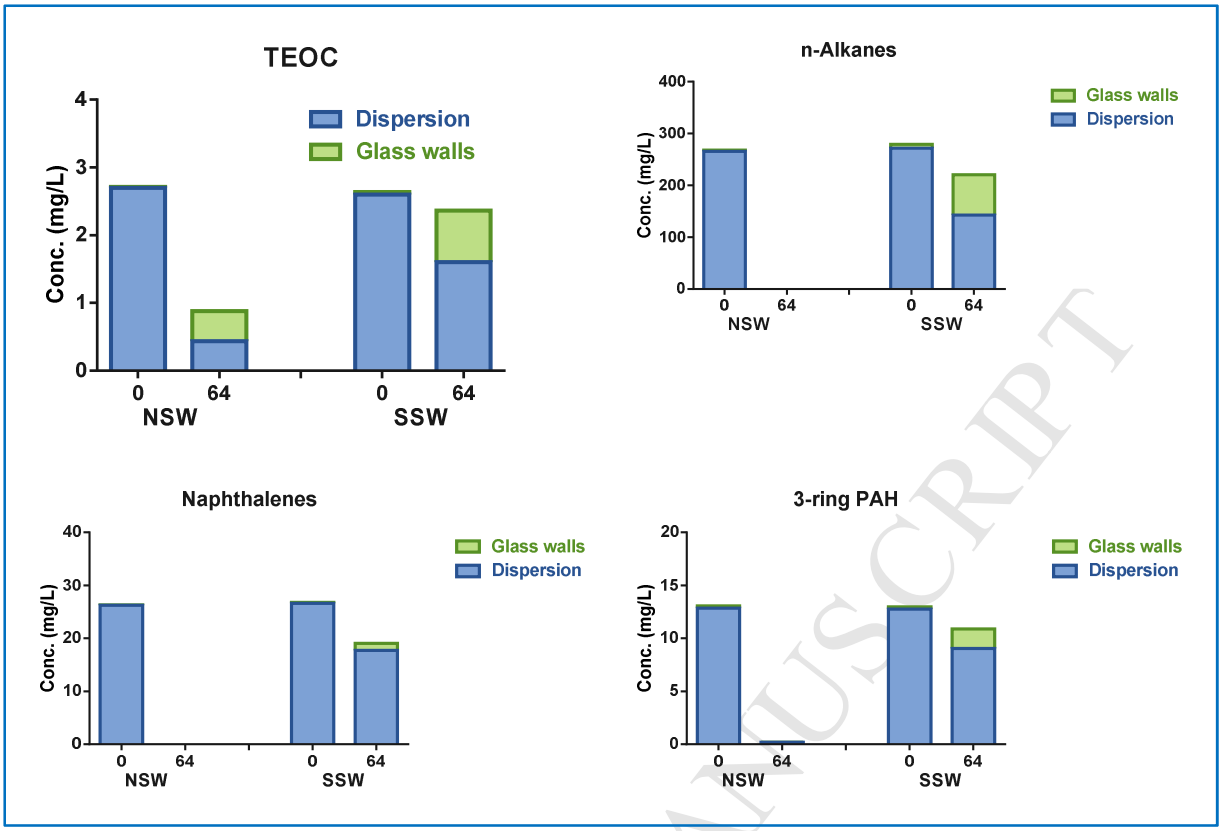

Fig. S5. Concentrations of TEOC, n-alkanes, naphthalenes and 3-ring PAH in dispersions and attached to the glass walls at the start (day 0) and termination (day 64) of an experiment with Statfjord oil premixed with Slickgone (DOR 1:100) and dispersed in the oil droplet generator. The dispersions were incubated (5°C) in natural SW (NSW) or in filtered and sterilized (100 mg/L $HgCl_2$) SW (SSW).

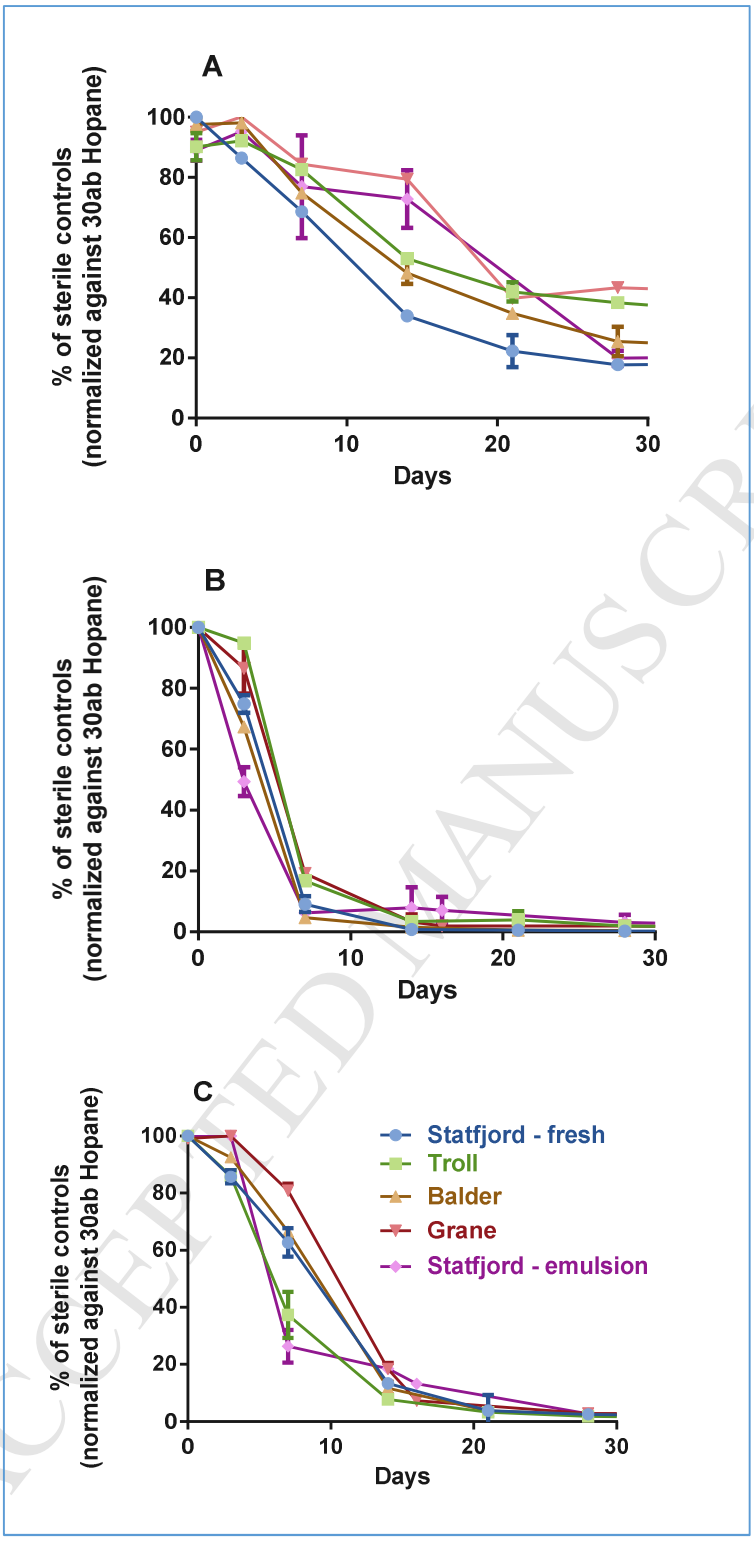

Fig. S6. Biotransformation of TEOC (A), sum nC_{10}-nC_{36} alkanes (B) and sum 2- 4-ring PAH in dispersions of different oils/emulsions. The results are shown as percentages in natural SW compared to in sterilized samples after normalization against 17α(H),21β(H)-Hopane (30ab Hopane). Error bars show standard deviations of 3 replicates.

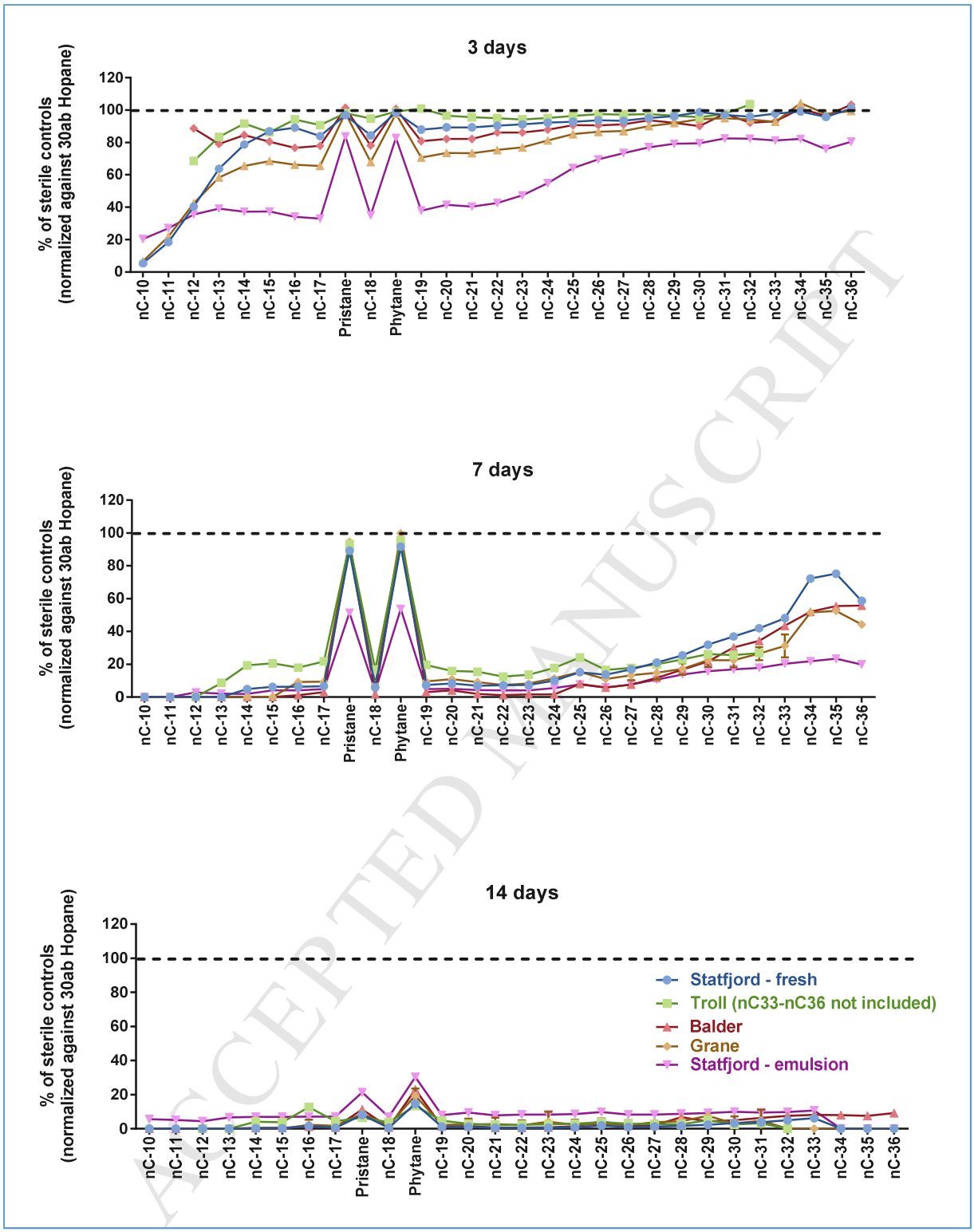

Fig. S7A. *n*-Alkane and isoprenoid (Pristane and Phytane) biodegradation between days 3 and 14 of the biodegradation study with chemically dispersed oils and emulsions. Each *n*-alkane concentration (average of replicates) was normalized against 17α(H),21β(H)-Hopane (30ab Hopane) and results shown as % of normalized concentrations of corresponding n-alkane in sterilized controls from same sampling days.

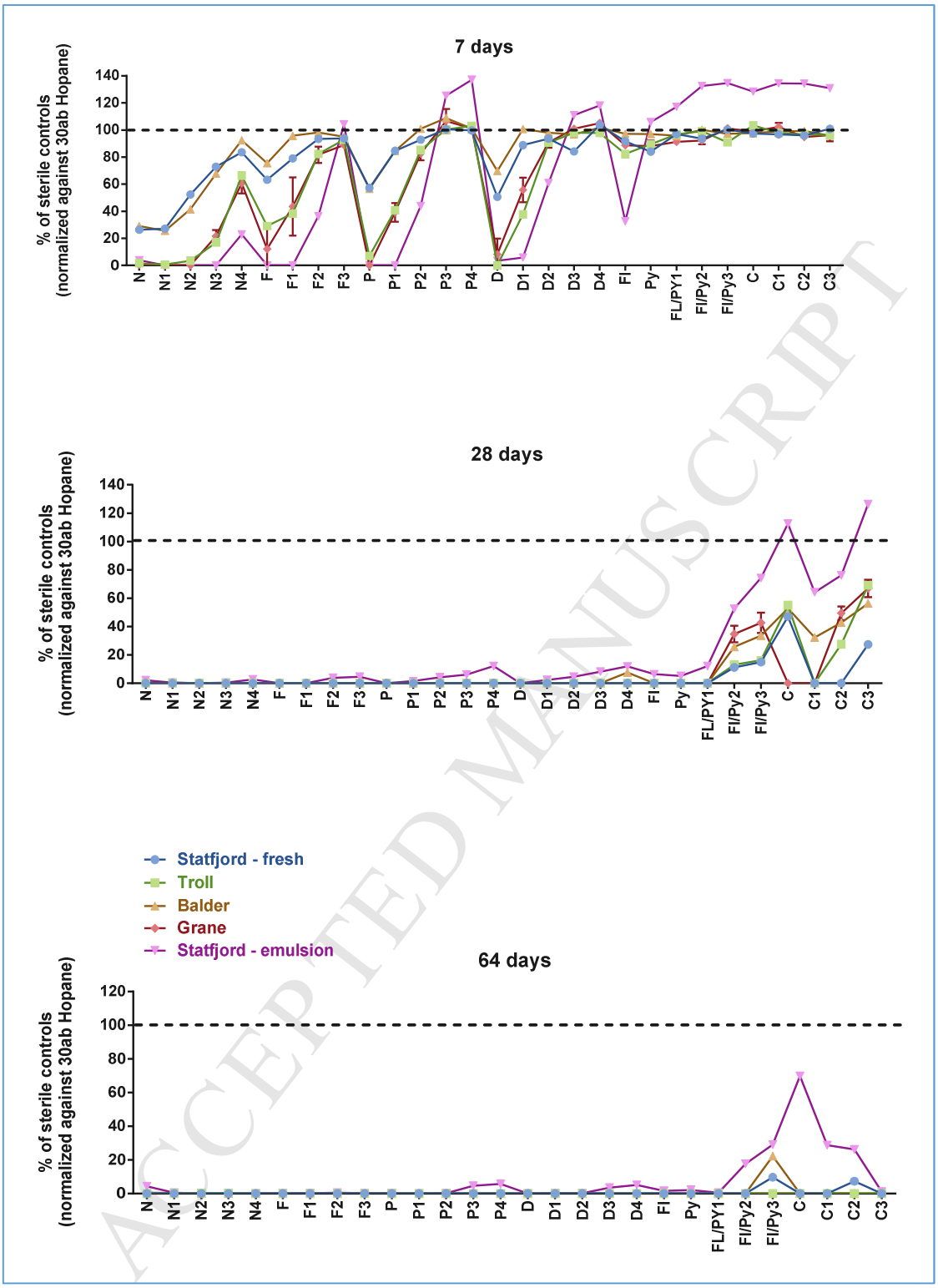

823

824 Fig. S7B. 2- to 4-ring PAH biotransformation between days 7 and 64 of the biodegradation
825 study with chemically dispersed oils and emulsions. The calculations of percentages of
826 sterilized controls are described above (Fig. S7A).

827

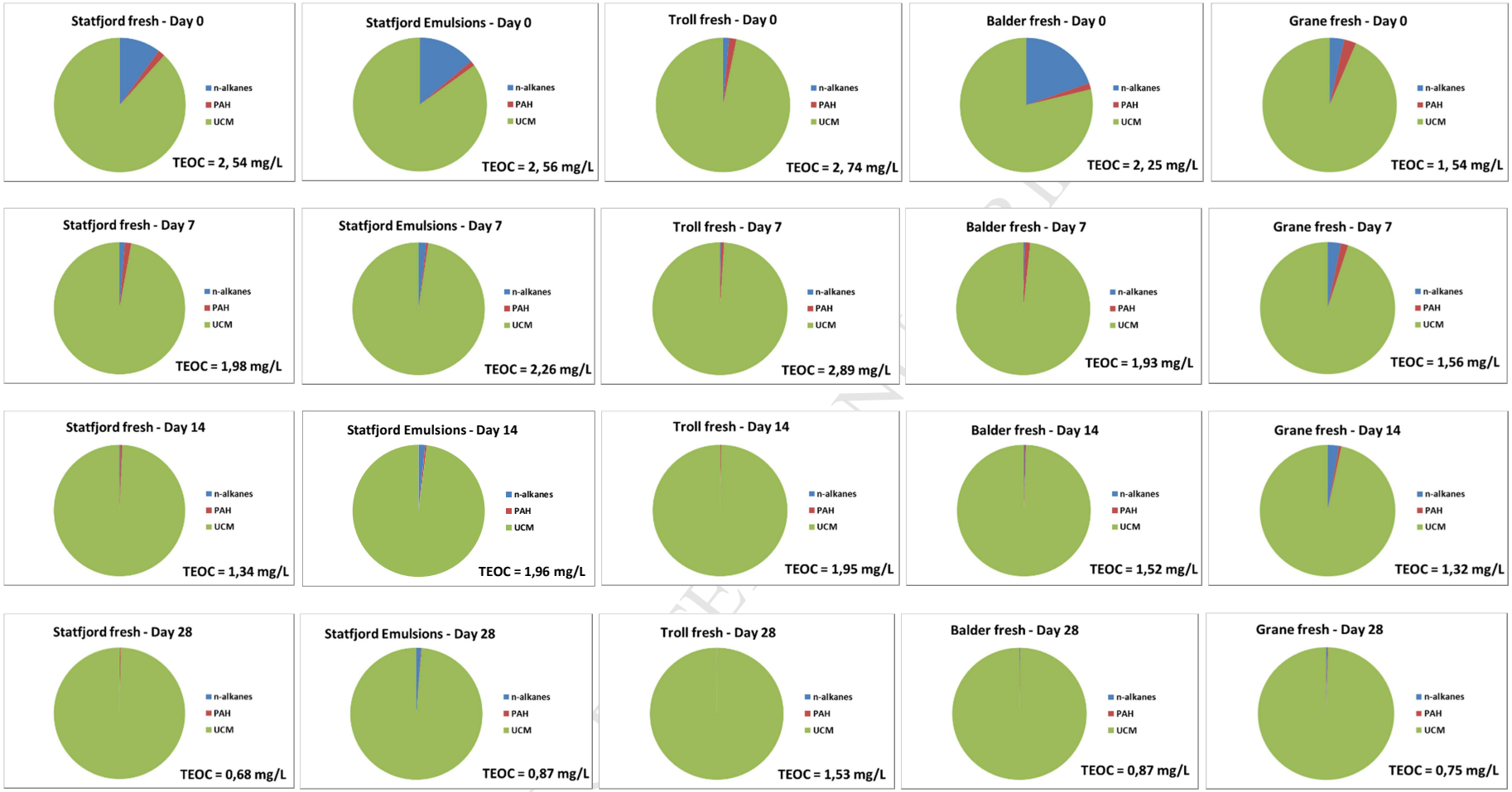

Fig. S8. TEOC concentrations and distribution between *n*-alkanes, PAH and UCM in the extracts during biodegradation.

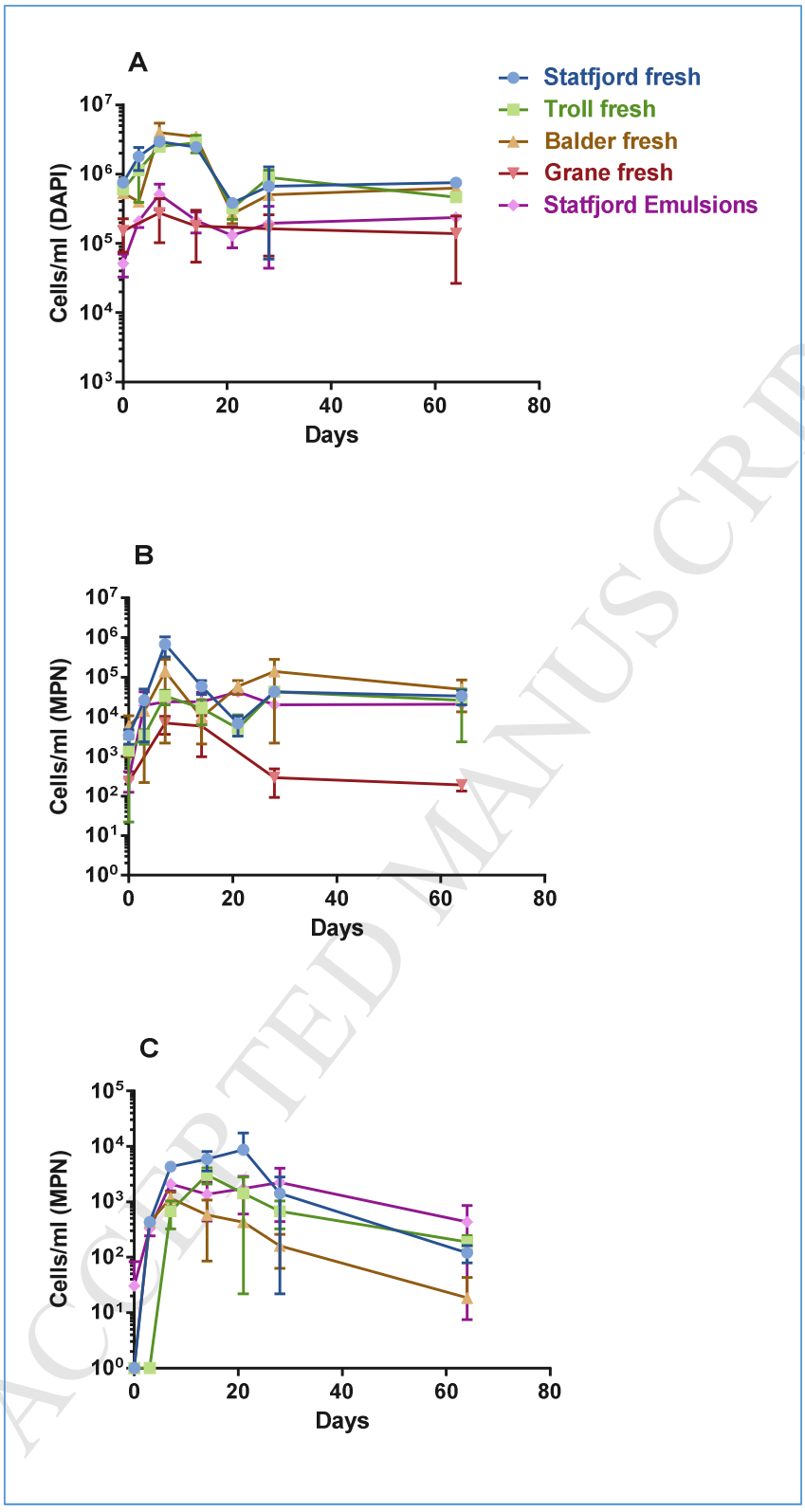

Fig. S9. Enumeration of total microbial concentrations (A), heterotrophic prokaryotes (B) and oil-degrading prokaryotes (C). Total concentrations were determined by epifluorescence microscopy after staining with DAPI, while heterotrophic and oil-degrading prokaryotes were determined by MPN. Error bars show standard deviations of 3 replicates (A), or 95 % confidence intervals (B and C).

Highlights

- Commercial dispersants efficiently dispersed crude oils with different properties
- IFT testing showed different surfactant leaching properties for oils and dispersants tested
- Biodegradation of alkanes and PAH did not differ significantly between the different oils
- Biodegradation of saturate and aromatic oil compound groups were provided for an oil spill model
- Oil biodegradation stimulated growth of heterotrophic and oil-degrading prokaryotes in all oils